Archives of Biochemistry and Biophysics
Vol. 399, No. 1, March 1, pp. 81–88, 2002
doi:10.1006/abbi.2001.2735, available online at http://www.idealibrary.com on IDEAL®

A Poplar Plastocyanin Mutant Suitable for Adsorption onto Gold Surface via Disulfide Bridge[1]

L. Andolfi,*,† S. Cannistraro,*,[2] G. W. Canters,† P. Facci,* A. G. Ficca,*
I. M. C. Van Amsterdam,† and M. Ph. Verbeet†,[2]

*INFM, Dipartimento di Scienze Ambientali, Università della Tuscia, I-01100 Viterbo, Italy; and
†Leiden Institute of Chemistry, Gorlaeus Laboratoria, Leiden University, The Netherlands

Received September 19, 2001, and in revised form November 20, 2001; published online February 7, 2002

Aiming to achieve stable immobilization for a redox-active cupredoxin protein onto a gold substrate and its consequent molecular level monitoring by Scanning Tunnelling Microscopy (STM), we introduced a disulphide bridge within poplar plastocyanin, while avoiding the perturbation of its active site. We selected and modified residues Ile-21 to Cys and Glu-25 to Cys by structurally conservative mutagenesis. Optical absorption spectroscopy (UV-Vis), electron paramagnetic resonance (EPR), and resonance raman scattering (RRS) results indicate that the active site of the Ile21Cys, Glu25Cys plastocyanin (PCSS) to a large extent retains the spectroscopic properties of the wild-type protein. Furthermore, the redox midpoint potential of the couple CuII/CuI in PCSS, determined by cyclic voltammetry was found to be +348 mV close to the wild-type value. The STM images display self-assembled PCSS molecules immobilised onto gold substrate. Moreover, the full potentiostatic control of the electron transfer reaction during STM imaging, suggests that the adsorbed molecule maintains essentially its native redox properties.

Key Words: **plastocyanin; type-1 copper site; disulfide linkage; site-directed mutagenesis; cupredoxins; metalloproteins.**

To study the self-assembling and electron transfer properties of metalloproteins and protoporphyrins (1–7), *in situ* STM has recently gained large popularity. For the metalloproteins, thiol groups and the disulfide bond appear to be suitable groups to chemisorb these proteins onto gold substrates. In this view the introduction of a disulfide bridge within poplar plastocyanin (PC),[3] which lacks an anchoring group for gold substrates, could provide for the possibility to achieve a stable immobilization of redox active protein onto gold substrate. The STM approach could open up the opportunity on one hand to study the electron transfer process in metalloproteins at the level of a single molecule, and on the other hand to investigate the electron transfer between a protein molecule and solid state electrodes. These issues represent an important task in developing concepts leading toward bioelectronic devices and biosensors (8).

Poplar Plastocyanin (PC) is a copper-binding protein of only 99 amino acids in size belonging to the cupredoxin family. PC is localized in the thylakoid lumen of the chloroplast and functions in photosynthesis as mobile electron carrier. PC is reduced by cytochrome *f*, which is part of the cytochrome b_6f complex, and oxidized by the reaction centre chlorophyll P700 of photosystem I. Despite some sequence divergence among plastocyanins derived from algae as compared to those from higher plants, the PCs overall three-dimensional structure is remarkably conserved (9).

PC (Fig. 1) is an eight-stranded, antipallalel β-sheet sandwich with a single copper ion coordinated by an $N_{\delta 1}$ from His-37 and His-87, an S_γ from Cys-84 and an

[1] The present work has been partly supported by a PRIN-MURST Project and by the EC Project SAMBA. L.A. acknowledges the INFM Advanced Research Project SINPROT.

[2] To whom correspondence and reprint requests should be addressed: Dr. M. Verbeet, Gorlaeus Labs, Einsteinweg 55, P.O. Box 9502, 2300-RA Leiden, The Netherlands. Fax: (31) 71 527 4593. E-mail: verbeet@chem.leidenuniv.nl; Professor Dr. S. Cannistraro, INFM, Dipartimento di Scienze Ambientali, Università della Tuscia, I-01100 Viterbo, Italy. Fax: +39 0761357136. E-mail: cannistr@unitus.it.

[3] Abbreviations used: PC, plastocyanin; UV-Vis, optical absorption spectroscopy; EPR, electron paramagnetic resonance; RRS, resonance raman scattering; PCSS, Ile21Cys, Glu25Cys plastocyanin; STM, scanning tunneling microscope.

0003-9861/02 $35.00

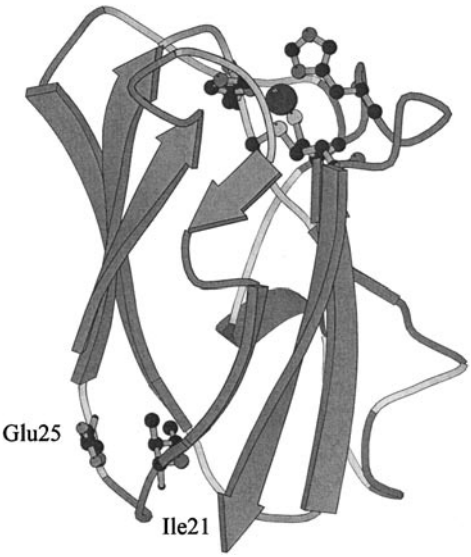

FIG. 1. The three-dimensional structure of poplar plastocyanin showing the copper atom at the top surrounded by the four ligands; i.e., starting from the top clockwise, His-87, Cys-84, Met-92, and His-37. The amino acid residues selected for the site-directed mutagenesis and the copper ligands are labelled. This drawing was generated by Molscript (37), using coordinates from file 1plc (35) in the Brookhaven Protein Data Bank.

S_δ from Met-92 in an irregular tetrahedral geometry (10). The copper site is at the Northern end of the molecule. The surface near this site consisting mainly of hydrophobic residues was termed "the hydrophobic patch." Another region located on the East side of the protein and containing many negatively charged side chains, i.e., glutamic and aspartic acid, is termed "the negative patch." These surface patches of the molecule are suggested to provide the interaction sites for the physiological donor and acceptor, respectively (9).

In PC, and generally in blue copper proteins, the copper site geometry is thought to be optimised for electron transfer mediation since minimal structural rearrangements are required for (CuII/I) redox cycling (11). It is believed that the electron transfer process occurs over relatively long distances and may involve bond- and space-tunneling mechanisms assisted by molecular vibrations (12).

The electron transfer process of PC and the interaction with its natural partners have been investigated with different spectroscopic approaches (13–15). In recent years, detailed structure–function studies of metalloproteins have taken advantage of the potentialities of site-directed mutagenesis. In the case of PC this technique has been used to modify the ligands of the Cu ion (16), and the residues of the negative and hydrophobic patches (17–19).

More recently, the electron transfer mechanism of azurin, a blue copper protein very similar to PC both in function and structure, have been investigated by *in situ* STM (1–6). Supposedly the disulfide bridge of azurin, which is surface exposed, mediates the adsorption of this protein onto gold (5, 6) and facilitates the electron tunnel routes between substrates and the tip via the copper ion (1, 2).

In order to extend the STM approach to PC, whose structural and functional aspects have been of main concern for the authors (20), we engineered a surface disulfide bridge opposite to the PC copper site (Fig. 1). This should provide the protein with an anchoring group, which is expected to direct the orientation of the protein redox site onto the gold electrode and thereby mimicking the aforementioned azurin gold adsorption.

In the first part of the present work we show that we succeeded in replacing both Ile21 and Glu25 with Cysteine. Subsequently, a spectroscopic characterisation showed that indeed the structure of the copper site closely resembles that of the wild-type protein. The PCSS redox potential, as determined by cyclic voltammetry, was found to be 348 mV, close to the wild-type value.

Finally, the STM imaging, under full potentiostatic control of the electron transfer reaction, revealed that PCSS self-assembles onto gold substrates, retaining its redox functionality.

MATERIAL AND METHODS

S–S Bond Program

The S–S bond program (21) was used to select suitable residues in PC for cystine generation.

Reagents, Bacterial Strain, and Plasmid

Restriction enzymes and DNA ligase were purchased from Pharmacia Biotech Inc. Primers for PCR were synthesised by Eurogentec (Belgium). For fragment isolation and purification the Gene Clean kit (BIO 101) was used.

Escherichia coli JM109 strain was used for the plasmid DNA manipulation, and *E. coli* HMS174 (DE3) from Novagen (U.S.A.) for the expression of both wild-type and mutated PC.

The parent plasmid, called pET3a-PC, a generous gift from Professor Hecht (Princeton, NJ), contains the synthetic gene encoding poplar plastocyanin inserted into the pET-3a expression vector (Novagen, Madison, WI). The gene, was inserted using *Nde*I and *Bam*HI restriction sites and expressed under the control of the T7 promoter (22). The gene construct does not encode a signal peptide sequence for periplasmatic targeting in bacterial cells. As a result the recombinant protein is expressed in the cytoplasm.

Mutagenesis

To generate the mutated gene, the isoleucine codon ATC at position 21 and the glutamate codon, GAG, at position 25 of the plastocyanin sequence had to be changed into cysteine codons TGC. Site-directed mutagenesis was carried out with a synthetic oligonucleotide that included the unique *Eco*RI site within the gene. The mutation primer had the sequence 5′CCGTCTGAATTCTCCTGCTCTCCCGGGTGCAAGATCGTGTTC-3′.

The mutant DNA fragment was created by a standard PCR amplification step involving the above mentioned pET3a-PC plasmid as

template and the mutation primer, the T7 terminator primer as the counter primer. The resulting PCR product consists of a fragment of 301 bp. The expression plasmid containing the mutations was constructed using the following steps: first, the 301-bp PCR product was digested with restriction enzymes Bpu1102 and *Eco*RI; second, one vector fragment of 432 bp, containing the T7 promoter, was obtained by digesting the vector pET3a-PC with restriction enzymes *Sal*I and *Eco*RI; finally another pET3a-PC fragment of 4204 bp, using the enzymes *Bpu*1102 and *Sal*I. Subsequently, the three purified fragments were ligated resulting in the vector pET3a-PCSS carrying the mutated gene. By DNA sequencing the PCSS mutations were confirmed (Baseclear, Leiden).

Protein Expression and Purification

The wild-type and the mutant PC were expressed in *E. coli* HMS174 (DE3). The cells harboring the expressing plasmids were grown at 37°C in 2× YT medium, supplemented with 100 μg/ml of ampicillin (or carbenicillin), and 0.1 mM copper citrate. The cells were grown in presence of copper citrate to improve the expression yield of copper protein (23). Upon reaching an OD_{600} = 1.0, protein production was induced by adding 0.2 mM IPTG. Growth was continued at 28°C for an additional 4 h. Bacterial cells were harvested by centrifugation at 7000*g* for 10 min at 4°C.

The PC was released from the bacterial cells by three freeze/thaw cycles (24). The supernatant resulting from a centrifugation of the cells (6000*g* for 10 min at 4°C) was dialysed against 0.5 mM $MgCl_2$ at 4°C, until a maximum amount of blue-colored PC was obtained. The dialysed sample was then loaded onto a DEAE Sepharose-fast flow (Pharmacia) column (preequilibrated with 20 mM sodium piperazine, pH 5.5). The protein was eluted at 30% of a salt gradient from 0 to 1 M NaCl (25).

In the case of the mutant protein, PCSS, following the dialysis of the supernatant with the released protein, a batchwise binding step using DEAE Sepharose was performed; subsequently the protein was eluted with 20 mM sodium phosphate at pH 6, 300 mM NaCl, to clarify the sample before the DEAE column chromatography step. Here, the PCSS protein was eluted using a linear salt gradient from 75 to 400 mM NaCl. As final purification step, the concentrated samples were run on Superdex 75 size-exclusion column in a Pharmacia FPLC set-up at a flow rate of 1 ml/min in a buffer containing 20 mM sodium phosphate, pH 6, 150 mM NaCl. The purity of the resulting samples was verified on a reducing SDS–PAGE and on an isoelectric focusing gel (PhastGel IEF 3-9 Pharmacia).

The N-terminal sequence and mass (by Electron Spray Mass spectroscopy) was determined for both wild-type PC and PCSS (Protein sequencing facility, LUMC, Leiden).

Analysis of the Disulfide Bond

The formation of the disulphide bridge was assessed by titrating free sulphydryls according to Ellman's method (26). For PCSS this determination was performed for the native form, both after oxidation and reduction, and for the denatured one. PCSS (20 μM) in a buffer containing an excess (25 μl of 4 mg/ml) 5,5′-dithiobis-2-nitrobenzoic acid (DTNB) in 20 mM sodium phosphate, pH 6, 150 mM NaCl was added to 0.1 M sodium phosphate, pH 8.0. The reaction of reduced, native PCSS was carried out after preincubation with 5 mM dithiotreitol (DTT) for 20 min at room temperature; then the sample was separated from DTT excess by filtration under nitrogen pressure against 0.1 M sodium phosphate, pH 6, in an Amicon minicell equipped with an YM3 ultrafiltration membrane (Millipore, Amicon).

For denaturation 6 M guanidinium hydrochloride (GdnHCl), 0.1 M sodium phosphate, pH 8.0, and 10 mM EDTA was added to 20 μM protein and 25 μl of DTNB. Subsequently, the number of free thiol groups was deduced spectroscopically from the increase in absorbance at 412 nm and calculated applying the ϵ_{412} values for the nitrothiobenzoate: 14150 $M^{-1}cm^{-1}$ in sodium phosphate buffer and 13700 $M^{-1}cm^{-1}$ in GdnHCl (27). The protein concentration was spectroscopically determined using an ϵ_{280} of 4200 $M^{-1}cm^{-1}$ (25).

Ultraviolet-Visible Spectroscopy

Optical absorbance spectra were recorded at room temperature by a double beam Jasco V-550 or Perkin–Elmer lambda-800 spectrophotometer. PCSS or PC in 20 mM sodium phosphate were placed in a quartz cuvette with 1 cm path length.

Resonance Raman Spectroscopy

The Resonance Raman spectrum of 0.8 mM of PCSS or PC in 20 mM sodium phosphate, pH 6.0, was recorded at room temperature, using a Dilor LaBram (ISA) Raman spectrometer. A HeNe 15 mW laser at 632.8 nm was used as the light source. The laser beam was directed by mirrors on an Olympus BX 40 microscope equipped with 4× objective having a 40 mm working distance. After filtering out of the laser line with a notch filter, the scattered light was dispersed with a 1800 line mm^{-1} holographic grating. A thermoelectrically cooled CCD array detector was used to record the Raman light. The spectrometer was calibrated using the silicon ν_1 line at 520.7 cm^{-1}.

Typical operating conditions were: 100 mW/mm^2 power density on the sample: 100 μm slit width; 3.0 cm^{-1} spectral width; acquisition time 120 s and 5 accumulations for each spectrum.

EPR Spectroscopy

The EPR spectra were recorded at 77 K on an X-band Varian E109 spectrometer. Therefore, 1 ml containing 0.17 mM for both proteins in 20 mM sodium phosphate, pH 6.0, was frozen in liquid nitrogen and placed in the cavity dewar. The spectrometer settings were: microwave power level 20 mW; time constant 0.25 s; modulation amplitude 0.0005 Tesla; modulation frequency 100 kHz; microwave frequency 9.084 GHz.

Cyclic Voltammetry

Polycrystalline gold electrodes were prepared by evaporating 150 nm of Au on freshly cleaved mica, in an evaporation system Minijev (High Vacuum Process) at 10^{-4} Pa. Cyclic voltammograms of 0.11 mM of PC and PCSS in 20 mM sodium phosphate, pH 6.0, were recorded with a Picostat potentiostat (Molecular Imaging Corporation, Phoenix, AZ). The electrochemical measurements were performed in a three standard electrode cell, where a saturated calomel electrode and a platinum wire were used as reference and counter, respectively.

STM Measurement

Substrates. Au (111) substrates were prepared by evaporating 50-nm-thick Au films onto freshly cleaved mica sheets. Au evaporation was performed at 0.5 nm/s deposition rate. After evaporation the films were left annealing at 450°C for 6 h and 10^{-5} Pa. After cooling down to room temperature, a moderate flame annealing was necessary to get large recrystallized Au (111) terraces.

Probes. STM tips were made from PtIr (80:20) by electrochemical etching of a 0.25 mm wire in a melt of $NaNO_3$ and NaOH. Tips were then insulated with molten Apiezon wax.

Preparation of the STM samples. Freshly prepared Au (111) substrates were incubated in 0.11 mM PCSS overnight at 4°C and then rinsed in abundant NH_4Ac buffer directly in the measuring cell, leaving always an aqueous layer on top of the substrate to prevent protein exposure to water surface tension. After several rinsing

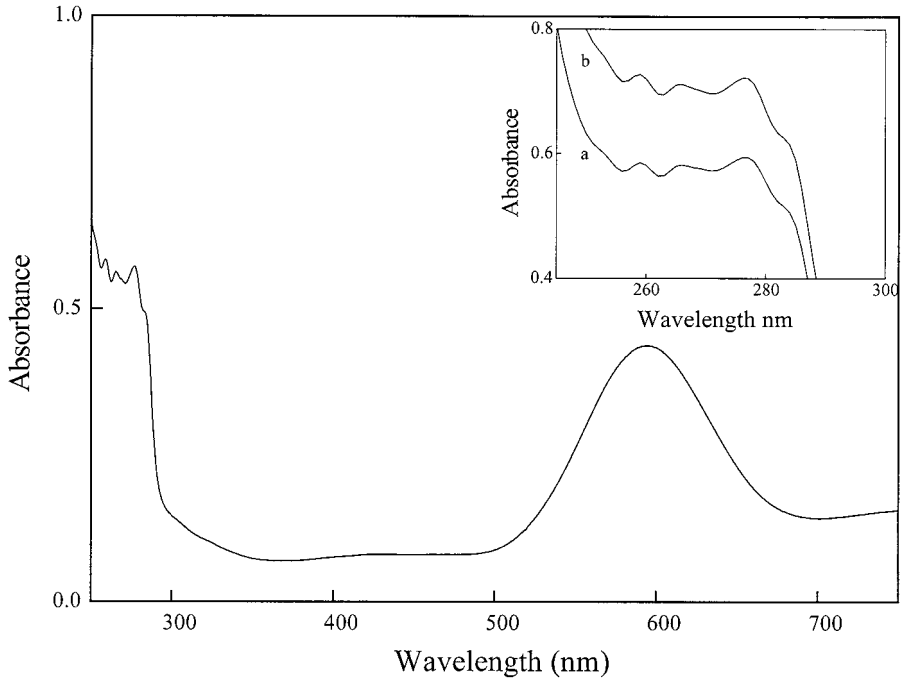

FIG. 2. The optical absorption spectrum of 0.11 mM PCSS in 20 mM sodium phosphate, pH 6.0. The inset displays the near -UV spectrum of the wild type PC (a) and PCSS (b).

cycles the measuring cell was filled with the same buffer and immediately installed in the microscope for imaging.

In situ STM. A Picoscan system (Molecular Imaging Co.) equipped with a Picostat (Molecular Imaging Co.) bipotentiostat was used to perform *in situ* STM investigation. The measuring cell consisted of a Teflon ring pressed over the Au (111) substrate operating as working electrode. A 0.5 mm Pt wire was used as counter electrode and a 0.5 mm Ag wire as quasireference electrode (AgQref). The AgQref potential was measured vs SCE before and after each experiment. In what follows the potentials will be always referred to SCE. In order to minimize buffer evaporation, the cell was mounted into a sealed Pirex chamber. Images were acquired at room temperature under electrochemical control at the potential of +28 mV at steady state current conditions.

A 10-μm scanner with a final preamplifier sensitivity of 1 nA/V was used for STM measurements. STM images were acquired in constant current mode with a typical tunneling current of 1 nA, bias voltage of 100 mV (tip positive), and scan rate of 2 Hz.

RESULTS AND DISCUSSION

The rationale for choosing the appropriate positions in PC for engineering a disulfide bridge, without impeding proper protein folding, was that the cysteine residues could establish a surface disulphide bond distant from the copper site. As a result this disulfide bridge would be available for an oriented self-assembly of PC on gold substrates. Among all the potential pairs of cysteine residues proposed by the S–S bond program (21), two possible combinations, i.e., Pro47-Gly78 and Ile21-Glu25, were taken into account. We ruled out the first one, because of the functional relevance of Pro47, placed in the β turn of PC, for the folding into the correct native structure (25). In the PC gene sequence we replaced the Ile-21 and the Glu-25 codons with Cys codons using PCR mutagenesis. The correct nucleotide sequence of the double mutant was established by DNA sequencing (not shown).

Both PCSS and PC were successfully expressed in the cytoplasm of *E. coli*. The mutant protein purification procedure differed slightly from that of the wild-type. For both proteins the isolation was carried out using the freeze/thaw method as recently developed by Hecht's group (24). In the case of wild-type PC, up to 90% of the overexpressed recombinant protein, with a size of approximately 11 kDa, is released from the host cells with a high degree of purity, without observing cellular lysis. In contrast, the PCSS (over-) expression resulted in more cellular lysis, presumably due to a toxic effect of the mutant protein on the cell stability. This also affected PCSS purification: upon dialysis, the supernatant was still viscous indicating contaminating lipids and chromatin material in the protein solution. These contaminants could be removed using a batch-wise binding step followed by elution from the anion exchange column. The purity of the resulting samples was verified on a reducing SDS–PAGE and on an isoelectric focusing gel. In both cases the protein ran as a single band on the gel.

The identity and integrity of PCSS was confirmed by subsequent characterisation using N-terminal sequencing and mass spectroscopy. Both N-terminal

amino acid sequences of PC and PCSS were identical with the N-terminal sequence published by Ybe and Hecht (22). Moreover, the presence of the cysteine residues in the expected positions 21 and 25 was established. The observed mass was in agreement with the expected molecular weight for PCSS (10578 ± 2 Da).

For investigating the disulphide bond formation we used the Ellman's reaction. The reaction was performed in the native form, both in the absence and in the presence of the reducing agent DTT. Under native conditions no free sulfhydryls were detected, whereas under denaturing conditions only the single free thiol group of the Cys84, which is among the four copper site ligands, was reactive with DNTB. From this, it can be inferred that the thiol groups of the inserted cysteines are not available for the reagent and therefore are involved in disulfide bond formation. Upon reduction of native form PCSS, 1.7 (±0.1) cysteine were titratable, indicating that both thiol groups are exposed. These results support that the thiol groups are accessible from the surface of PCSS and that the formation of the disulfide bond has occurred. Recently, the presence of the disulphide bond in the PCSS was confirmed by obtaining its 3-D crystal structure (28).

Since the cytoplasm of the bacteria is supposed to be a reducing environment, the disulfide bond probably becomes established upon exposure to an oxidising environment during release of the protein from the cells.

In order to investigate if the introduced disulfide bridge affects the special structure of the redox active site, which is crucial for the functionality of PC, the mutant was first spectroscopically characterised. Figure 2 shows the absorption of oxidized PCSS in the UV-visible range. The presence of the intense band at 597 nm, that corresponds to the cysteine sulfur-to-copper transition in which an electron is promoted from the Cu-S bonding orbital to the π^* antibonding orbital (29), shows that the copper site of the mutant maintains the same electronic structure as the wild-type. The near UV-region, as shown in the inset of Fig. 2, displays that the fine structure of PCSS (b) is identical to PC (a). The peaks and shoulders in the near-UV region of poplar PC can be attributed to tyrosine and phenylalanine residues (30). The absorption spectrum of this region indicates that no significant changes in the local environment of these aromatic residues can be detected as consequence of the mutation. A value of 1.1 for the ratio A_{280}/A_{597}, both for PC and PCSS, has been obtained, indicating similar properties and purity for both protein preparations.

Figure 3 shows the EPR spectra of PC (a) and PCSS (b). For both samples the spectral features are consistent with a distorted copper site geometry of PC, with the four hyperfine lines centred at $g_\parallel$, separated by $A_\parallel$, and a single more intense resonance line centred at $g_\perp$, at higher field. The $g_\perp \sim 2.074$, $g_\parallel \sim 2.265$, and the $A_\parallel \sim 65.6 \times 10^{-4}$ cm^{-1} displayed by the mutant, are slightly different with respect to the $g_\perp \sim 2.078$, $g_\parallel \sim 2.269$, and the $A_\parallel \sim 61.4 \times 10^{-4}$ cm^{-1} of the wild-type. However, the measured values both for wild-type and mutant are in general agreement with the literature (31).

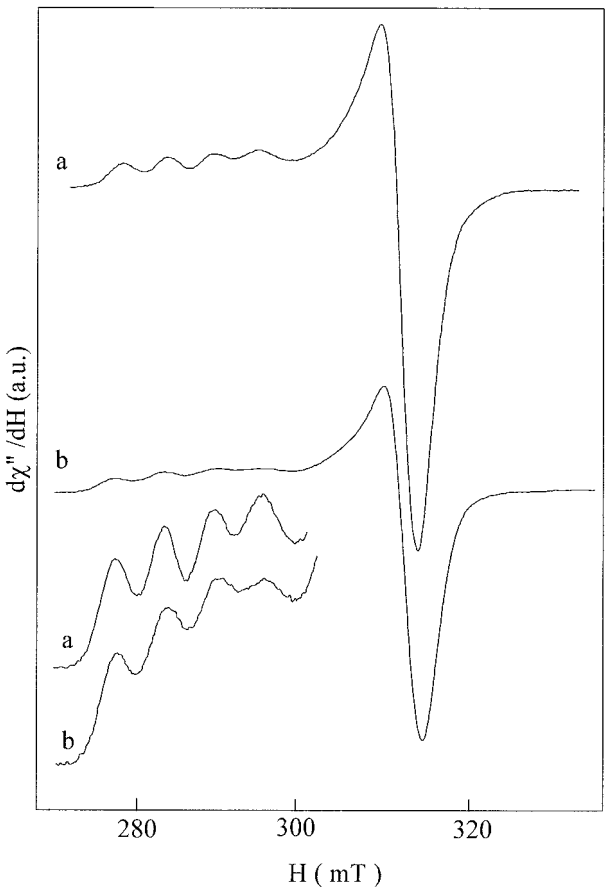

FIG. 3. EPR spectra of the wild-type PC (a) and PCSS (b). The wild-type sample contains 0.17 mM of protein in 20 mM sodium phosphate, pH 6.0; the Cu^{2+} content is estimated to be 0.12 mM. The PCSS sample contains 0.17 mM of protein in 20 mM sodium phosphate pH 6.0 and the Cu^{2+} content is estimated to be 0.08 mM. The inset shows the corresponding parallel pattern of the PC (a) and PCSS (b) at higher gain.

The low field hyperfine pattern centred at $g_\parallel$, see inset of Fig. 3, displays a distortion, that consists of different shapes and heights of the copper hyperfine lines and an unequal spacing between adjacent lines. In addition, the PCSS spectrum shows also a different height of the last hyperfine lines at high magnetic field. Presumably, such an effect, already observed in many metalloproteins, is due to heterogeneity in the site geometry, termed "strain effect" (32, 33). The difference in the EPR signals intensities are due to a different Cu^{2+} concentration in the two samples, as indicated in the legend of Fig. 3.

Information about the vibrational properties of the copper site were provided by RR spectroscopy. In

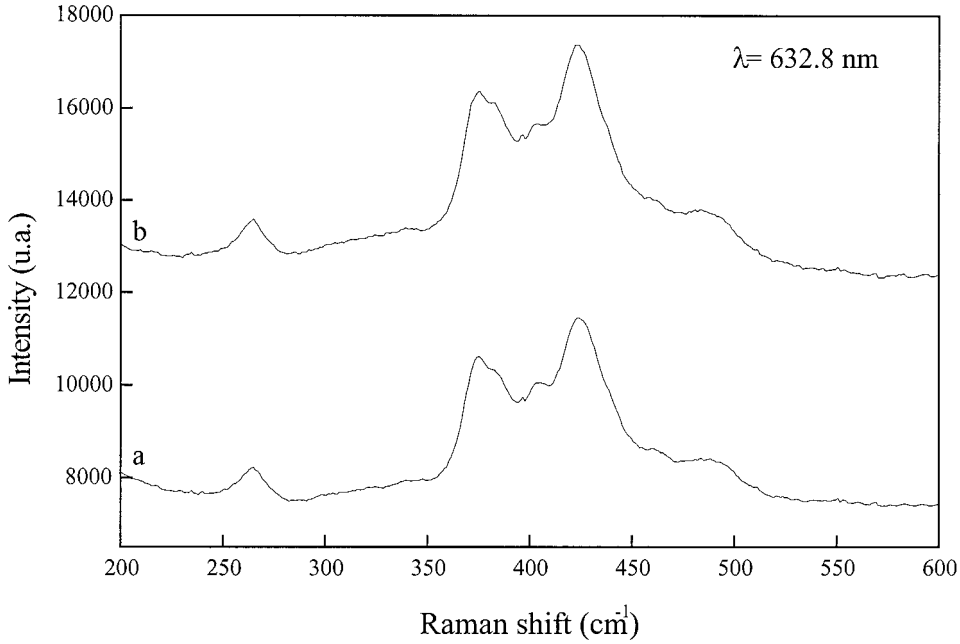

FIG. 4. Resonance Raman spectra of 0.8 mM of wild type (a) and PCSS (b) in 20 mM sodium phosphate, pH 6.0, excited at 632.8 nm at room temperature.

Fig. 4, room temperature RR spectra of PC (a) and PCSS (b) obtained with excitation at 632.8 nm, are shown. Both spectra display the typical intense bands between 350 and 500 cm^{-1} and a moderately intense band at 266 cm^{-1}, which for wild-type PC, have been previously assigned to the vibrational modes involving the Cu-S stretch mixed with other vibrational modes and to the symmetric Cu-N stretch from the histidine ligands (34). The close similarity between the two RR spectra, suggests that the mutant maintains the structure and dynamics of the copper active site similar to that of wild-type protein. Finally, to complete the information about the copper site properties we investigated the redox behavior of PC and PCSS by cyclic voltammetry. The midpoint potentials determined for the wild-type (+83 mV) and PCSS (+106 mV) were found to be slightly different, but within the experimental error.

The adsorption of the PC mutant onto gold substrates was performed at pH 4.6. This pH value, close

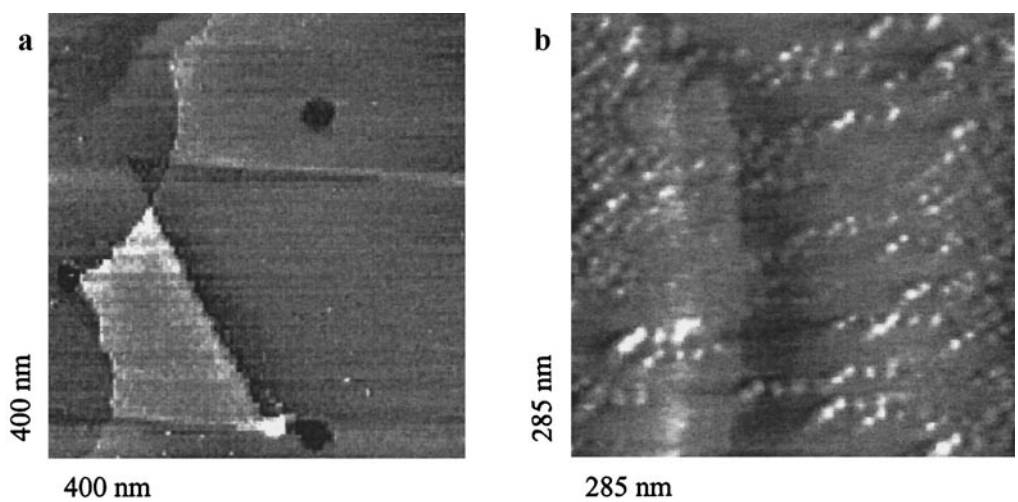

FIG. 5. Constant current image of bare Au (111) terraces, scan area 400 × 400 nm^2 (a) and PCSS adsorbed onto Au (111) substrate, scan area 285 × 285 nm^2 (b) in 50 mM ammonium acetate, pH 4.6, measured by *in situ* electrochemical STM.

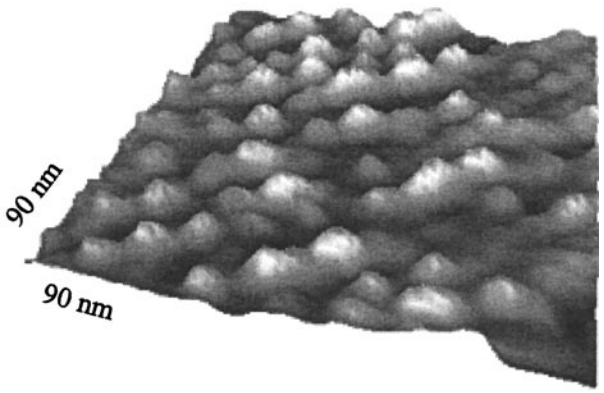

FIG. 6. Three-dimensional STM view showing PCSS adsorbed on Au (111) recorded in 50 mM ammonium acetate, pH 4.6, by *in situ* electrochemical STM in constant-current mode. Image corrugation is 0.8 nm. Scan area 90 × 90 nm^2.

to the isoelectric point of the PCSS (p*I* 4.39), was chosen to minimise possible charge interaction between surface immobilized protein and the ones coming to the substrate. Figure 5 shows representative STM images acquired at a substrate potential of +28 mV. In Fig. 5a the flat terraces of Au (111) are shown. In Fig. 5b, after the incubation with PCSS protein solution, bright spots appear on the gold substrate. The spots have a lateral size of 3–4 nm, which is in agreement with the crystallographic dimension of the PC (28, 35). Concerning the depth (z-axis), we found a dimension of about 0.8 nm, which is smaller than the actual crystallographic dimension. Such a discrepancy is, however, a common feature in protein adsorbed onto gold and imaged by STM (2, 36). Figure 6 displays a zoomed three-dimensional view with a dense coverage. The image shows an uniform corrugation, which is characterized by a highly ordered array. *In situ* STM imaging for PCSS appears to be robust and repeatable at molecular resolution, suggesting that a stable adsorption of the mutant protein via disulphide bond onto the gold substrate is involved. Indeed, this linking was inferred also from equivalent experiments carried out with the wild-type PC. Only a low coverage of spots was noticed irregular in size, which yielded for the wild-type PC a less stable imaging (data not shown). These features can be easily interpreted as a physical adsorption of the wild-type protein onto the Au (111) surface. Consequently, in the case of wild-type PC this lack of stability in imaging indicates that neither stable nor oriented adsorption takes place. From the results above we can conclude that a stable immobilisation of PCSS is reached via disulphide bond, leading at the same time to a well defined orientation of PCSS redox centre on the substrate. These fully potentiostatically controled *in situ* STM images reveal that no denaturation of the PCSS has occurred as consequence of the protein–metal interaction and that protein redox properties are preserved. Considering the images obtained in this study we can further suggest that the PCSS behaves much alike azurin, both for self-assembling properties and for the stability of imaging (1–6).

In conclusion, in this work we have generated a second cupredoxin like molecule to broaden the understanding of the redox activity of the type I copper protein at level of single molecule.

ACKNOWLEDGMENTS

We are grateful to Professor M. H. Hecht (Princeton, U.S.A.) for supplying the plasmid pET3a containing the poplar PC gene and Professor B. Hazes (University of Groningen, Netherlands) for providing the SS bond program.

REFERENCES

1. Friis, E. P., Andersen, J. E. T., Madsen, L. L., Moller, P., and Ulstrup, J. (1997) *J. Electroanal. Chem.* **431,** 35–38.
2. Friis, E. P., Andersen, J. E. T., Kharkats, Y. I., Kuznestov, A. M., Nichols, R. J., Zhang, J. D., and Ulstrup, J. (1999) *Proc. Natl. Acad. Sci. USA* **96,** 1379–1384.
3. Davis, J. J., Halliwell, C. M., A. O. H., Hill, Canters, G. W., Van Amsterdam, M. C., and Verbeet, M. Ph. (1998) *New J. Chem.* **22,** 1119–1123.
4. Friis, E. P., Andersen, E. T. J., Madsen, L. L., Møller, P., Nicholson, R. J., Olesen, K. G., and Ulstrup, J. (1998) *Electrochimica Acta* **43,** 2889–2897.
5. Chi, Q., Zhang, J., Nielsen, J. U., Friis, E. P., Chorkendorff, Ib., Canters, G. W., Andersen, J. E. T., and Ulstrup, J. (2000) *J. Am. Chem. Soc.* **122,** 4047–4055.
6. Facci, P., Alliata, D., and Cannistraro, S. (2001) *Ultramicroscopy* **89,** 291–298.
7. Tao, N. J. (1996) *Phys. Chem. Rev. Lett.* **76,** 4066–4069.
8. Molecular Electronics-Science and Technology (Aviram, A., Ed.) AIP, New York, 1992; C. A., Mirkin, M. A., Ratner, (1992) *Annu. Rev. Phys. Chem.* **43,** 719.
9. Redinbo, M. R., Yeates, T. O., and Merchant, S. (1994) *J. Bioenerg. Biomemb.* **26,** 49–66.
10. Guss, J. M., and Freeman, H. C. (1983) *J. Mol. Biol.* **169,** 521–563.
11. Shepard, W. E. B., Anderson, B. F., Lewandoski, D. A., Norris, G. E., and Baker, E. N. (1990) *J. Am. Chem. Soc.* **112,** 7817–7819.
12. Skourtis, S. S., and Beratan, D. N. (1997) *J. Biol. Inorg. Chem.* **2,** 378–386.
13. Faver, O., Shahak, Y., and Pecht, I. (1982) *Biochemistry* **21,** 1885–1890.
14. Takabe, T., Ishikawa, H., Niwa, S., and Itoh, S. (1983) *J. Biochem.* **94,** 1901–1911.
15. Olsen, L. F. (1982) *Biochimica Biophysica Acta.* **682,** 482–490.
16. Hibino, T., Lee, B. H., Takabe, T., and Takabe, T. (1995) *J. Biochem.* **117,** 101–106.
17. Olesen, K., Ejdebäck, M., Crnogorac, M. M., Kostic, N. M., and Hansson, Ö. (1999) *Biochemistry* **38,** 16695–16705.
18. Sigfridsson, K., Young, S., and Hansson, Ö. (1997) *Eur. J. Biochem.* **245,** 805–812.

19. Sigfridsson, K., Young, S., and Hansson, Ö. (1996) *Biochemistry* **35,** 1249–1257.
20. Wang, C. X., Bizzarri, A. R., Xu, Y. W., and Cannistraro, S. (1994) *Chem. Phys.* **183,** 155–166; Bizzarri, A. R., Xang, C., Chen, W. Z., and Cannistraro, S. (1995) *Chem. Phys.* **201,** 463–472; Guzzi, R., Bizzarri, A. R., Sportelli, L., and Cannistraro, S. (1997) *Biophysical Chem.* **214,** 211–219; Rocchi, C., Bizzarri, A. R., and Cannistraro, S. (1997) *Chem. Phys.* **214,** 261–276; Ciocchetti, A., Bizzarri, A. R., and Cannistraro, S. (1997) *Biophys. Chem.* **69,** 185–198; Arcangeli, C., Bizzarri, A. R., and Cannistraro, S. (1998) *Chem. Phys. Lett.* **291,** 7–14; Bizzarri, A. R., and Cannistraro, S. (1999) *Phisyca A* **267,** 257–270; Bizzarri, A. R., Paciaroni, A., and Cannistraro, S. (2000) *Phys. Rev. E* **62,** 3991–3999.
21. Hazes, B., and Dijkstra, B. W. (1988) *Protein Eng.* **2,** 119–125.
22. Ybe, J. A., and Hecht, M. H. (1994) *Protein Express. Purif.* **5,** 317–323.
23. Qiu, D., Dong, S., Ybe J. A., Hecht, M. H., and Spiro, T. (1994) *J. Am. Chem. Soc.* **117,** 6443–6446.
24. Johnson, B. H., and Hecht, M. H. (1994) *Bio/Technology* **12,** 1357–1360.
25. Ybe, J. A., and Hecht, M. H. (1996) *Protein Sci.* **5,** 814–824.
26. Ellman, G. L. (1959) *Arch. Biochem. Biophys.* **82,** 70–77.
27. Aitken, A., and Learmonth, M. (1996) *in* The Protein Protocol Handbook (Walker J. M., Ed.), pp. 487–488, Humana Press, Totowa, NJ.
28. Milani, M., Andolfi, L., Cannistraro, S., Verbeet, M. Ph, and Bolognesi, M. (2001) *Acta Crystallogr. D* **57,** 1735–1738.
29. Penfield, K. W., Gewirth, A. A., and Solomon, E. I. (1985) *J. Am. Chem.* **107,** 4519–4529.
30. Donovan, J. W. (1979) *in* Physical Principles and Techniques in Protein Chemistry (Leach, S. J., Ed.), part A, pp. 102–170, Academic Press, New York.
31. Holm, R. H., Kennepohl, P., and Solomon, E. I. (1996) *Chem. Rev.* **96,** 2239–2314.
32. Cannistraro, S. (1990) *J. Phys. Fr.* **51,** 131–139; Bizzarri, A. R., and Cannistraro, S. (1995) *Mol. Phys.* **85,** 913–929.
33. Groeneveld, C. M., Aasa, R., Reinhammar, B., and Canters, G. W. (1987) *J. Inorg. Biochem.* **31,** 143–154.
34. Fraga, E., Webb, M. A., and Lopponow, G. R. (1996) *J. Phys. Chem.* **100,** 3278–3287.
35. Guss, J. M., Bartunik, H. D., and Freeman, H. C. (1992) *Acta Crysallogr. B* **48,** 790–811.
36. Davis, J. J., Djricic, D., Lo, K. W. K., Wallace, E. N. K., Wong, L. L., and Hill, H. A. O. (2000) *Faraday Discuss.* **116,** 15–22.
37. Kraulis, P. J. (1991) *J. Appl. Crystallogr.* **24,** 946–950.